Determining the Higgs Spin and Parity in the Diphoton Decay Channel

Daniël Boer,[1] Wilco J. den Dunnen,[2] Cristian Pisano,[3] and Marc Schlegel[2]

[1]*Theory Group, KVI, University of Groningen, Zernikelaan 25, NL-9747 AA Groningen, The Netherlands*
[2]*Institute for Theoretical Physics, Universität Tübingen, Auf der Morgenstelle 14, D-72076 Tübingen, Germany*
[3]*Dipartimento di Fisica, Università di Cagliari, and INFN, Sezione di Cagliari, I-09042 Monserrato (CA), Italy*

(Received 19 April 2013; published 18 July 2013)

We calculate the diphoton distribution in the decay of arbitrary spin-0 and spin-2 bosons produced from gluon fusion, taking into account the fact that gluons inside an unpolarized proton are generally linearly polarized. The gluon polarization brings about a difference in the transverse momentum distribution of positive and negative parity states. At the same time, it causes the azimuthal distribution of the photon pair to be nonisotropic for several spin-2 coupling hypotheses, allowing one to distinguish these from the isotropic scalar and pseudoscalar distributions.

DOI: 10.1103/PhysRevLett.111.032002 PACS numbers: 12.38.−t, 13.85.Ni, 13.88.+e, 14.80.Bn

Last year in July it was announced that a new boson with a mass of around 125–126 GeV was observed by both the ATLAS [1] and CMS [2] collaborations. An excess of events was observed in $\gamma\gamma$, ZZ^*, and WW^* production from proton-proton collisions at a center of mass energy ($\sqrt{s}$) of 7 and 8 TeV. The observed excess is consistent, within uncertainties, with the production and decay of the standard model Higgs boson.

Now that the existence of a new particle has been established, both collaborations have begun the determination of its spin and parity. Both ATLAS [3–5] and CMS [6–8] set approximately 3 σ exclusions on the $J^P = 0^-$ scenario using the ZZ^* channel, while the 2^+_m hypothesis [9] starts to be disfavored at 1–3 σ in the $\gamma\gamma$, ZZ^*, and WW^* channels. As the decay of a pure spin-1 state to two photons is not allowed according to the Landau-Yang theorem [10,11], the $\gamma\gamma$ channel is being used to distinguish between spin 0 and spin 2 only. In the ZZ^* and WW^* channels, the spin-1 option should also be considered.

Even though the number of events is much larger in the $\gamma\gamma$ channel, the ability to distinguish spin 0 from spin 2 is *not* much better than in the ZZ^* channel. The reason is that in the $\gamma\gamma$ channel only the distribution of the polar angle θ is considered [3,12–16]. The spin-0 and spin-2 hypotheses are not very different in this variable after experimental acceptance cuts [3], leading to a small discriminating power. The determination of the parity using only this angle is even impossible, as the distributions of 0^+ and 0^- are exactly equal and the same holds true for the $2^\pm_h$ scenarios [17].

In this Letter we demonstrate that one can also differentiate between the different spin scenarios in the $\gamma\gamma$ channel, by studying the dependence on the *azimuthal* angle ϕ in the Collins-Soper frame [18], which is the diphoton rest frame with the $\hat{x}\hat{z}$ plane spanned by the 3-momenta of the colliding protons and the $\hat{x}$ axis set by their bisector. Moreover, different spin-2 coupling hypotheses that have an equal θ dependence can be distinguished from each other using the ϕ distribution, enhancing the analyzing potential of this channel. Apart from that, we update predictions for the transverse momentum distribution [19,20] which can, in principle, be used to distinguish the different parity states 0^+ from 0^- and 2^+_h from 2^-_h in the $\gamma\gamma$ channel. Azimuthal angular distributions have been discussed for spin-0 and spin-2 ''Higgs'' production from vector-boson fusion [21–23], but not yet from gluon fusion and not including linear polarization.

A nontrivial ϕ distribution in the decay of spin-2 bosons produced from gluon fusion can be caused by the fact that gluons in an unpolarized proton are generally linearly polarized. The degree of gluon polarization can be calculated using perturbative quantum chromodynamics (pQCD) for transverse momentum of the gluon much larger than the proton mass and is found to be large. For small transverse momentum pQCD cannot be used to calculate the degree of polarization, but this lack of knowledge turns out to be of little influence on the final ϕ distribution, which is mostly dominated by the perturbative part.

The effects of gluon polarization can be described in the framework of transverse momentum dependent (TMD) factorization. In that framework, the full $pp \to \gamma\gamma X$ cross section is split into a partonic $gg \to \gamma\gamma$ cross section and two TMD gluon correlators, which describe the distribution of gluons inside a proton as a function of not only its momentum along the direction of the proton, but also transverse to it. More specifically, the differential cross section for the inclusive production of a photon pair from gluon-gluon fusion is written as [24,25],

$$\frac{d\sigma}{d^4q\,d\Omega} \propto \int d^2\boldsymbol{p}_T d^2\boldsymbol{k}_T \delta^2(\boldsymbol{p}_T + \boldsymbol{k}_T - \boldsymbol{q}_T)\mathcal{M}_{\mu\rho\kappa\lambda}(\mathcal{M}_{\nu\sigma}{}^{\kappa\lambda})^* \Phi_g^{\mu\nu}(x_1, \boldsymbol{p}_T, \zeta_1, \mu)\Phi_g^{\rho\sigma}(x_2, \boldsymbol{k}_T, \zeta_2, \mu), \quad (1)$$

with the longitudinal momentum fractions $x_1 = q \cdot P_2/P_1 \cdot P_2$ and $x_2 = q \cdot P_1/P_1 \cdot P_2$, q the momentum of the photon pair, $\mathcal{M}$ the $gg \to \gamma\gamma$ partonic hard scattering matrix element and Φ the following unpolarized proton gluon TMD correlator,

$$\Phi_g^{\mu\nu}(x, \boldsymbol{p}_T, \zeta, \mu) \equiv 2 \int \frac{d(\xi \cdot P) d^2\xi_T}{(xP \cdot n)^2 (2\pi)^3} e^{i(xP+p_T)\cdot\xi} \mathrm{Tr}_c[\langle P|F^{n\nu}(0)\mathcal{U}^{n[-]}_{[0,\xi]} F^{n\mu}(\xi)\mathcal{U}^{n[-]}_{[\xi,0]}|P\rangle]_{\xi\cdot P'=0}$$
$$= -\frac{1}{2x}\left\{g_T^{\mu\nu} f_1^g(x, \boldsymbol{p}_T^2, \zeta, \mu) - \left(\frac{p_T^\mu p_T^\nu}{M_p^2} + g_T^{\mu\nu}\frac{\boldsymbol{p}_T^2}{2M_p^2}\right) h_1^{\perp g}(x, \boldsymbol{p}_T^2, \zeta, \mu)\right\} + \mathrm{HT}, \quad (2)$$

with $p_T^2 = -\boldsymbol{p}_T^2$ and $g_T^{\mu\nu} = g^{\mu\nu} - P^\mu P'^\nu/P \cdot P' - P'^\mu P^\nu/P \cdot P'$, where P and P' are the momenta of the colliding protons and M_p their mass. The gauge link $\mathcal{U}^{n[-]}_{[0,\xi]}$ for this process arises from initial state interactions. It runs from 0 to ξ via minus infinity along the direction n, which is a timelike dimensionless four vector with no transverse components such that $\zeta^2 = (2n \cdot P)^2/n^2$. In principle, Eqs. (1) and (2) also contain soft factors, but with the appropriate choice of ζ (of around 1.5 times $\sqrt{s}$), one can neglect their contribution, at least up to next-to-leading order [25,26]. To avoid the appearance of large logarithms in $\mathcal{M}$, the renormalization scale μ needs to be of order M_h. The last line of Eq. (2) contains the parametrization of the TMD correlator in terms of the unpolarized gluon distribution f_1^g, the linearly polarized gluon distribution $h_1^{\perp g}$, and higher twist (HT) terms, which only give $\mathcal{O}(1/Q)$ suppressed contributions to the cross section, where $Q \equiv \sqrt{q^2}$.

The general structure of the differential cross section for the process $pp \to \gamma\gamma X$ is given by [27]

$$\frac{d\sigma}{d^4q d\Omega} \propto F_1(Q,\theta)\mathcal{C}[f_1^g f_1^g] + F_2(Q,\theta)\mathcal{C}[w_2 h_1^{\perp g} h_1^{\perp g}]$$
$$+ F_3(Q,\theta)\mathcal{C}[w_3 f_1^g h_1^{\perp g} + (x_1 \leftrightarrow x_2)]\cos(2\phi)$$
$$+ F_3'(Q,\theta)\mathcal{C}[w_3 f_1^g h_1^{\perp g} - (x_1 \leftrightarrow x_2)]\sin(2\phi)$$
$$+ F_4(Q,\theta)\mathcal{C}[w_4 h_1^{\perp g} h_1^{\perp g}]\cos(4\phi) + \mathcal{O}(q_T^2/Q^2), \quad (3)$$

where the F_i factors consist of specific combinations of $gg \to X_{0,2} \to \gamma\gamma$ helicity amplitudes, with $F_{3,4}$ involving amplitudes with opposite gluon helicities. The convolution $\mathcal{C}$ is defined as

$$\mathcal{C}[wfg] \equiv \int d^2\boldsymbol{p}_T \int d^2\boldsymbol{k}_T \delta^2(\boldsymbol{p}_T + \boldsymbol{k}_T - \boldsymbol{q}_T)$$
$$\times w(\boldsymbol{p}_T, \boldsymbol{k}_T) f(x_1, \boldsymbol{p}_T^2) g(x_2, \boldsymbol{k}_T^2) \quad (4)$$

and the weights appearing in the convolutions as

$$w_2 \equiv \frac{2(\boldsymbol{k}_T \cdot \boldsymbol{p}_T)^2 - \boldsymbol{k}_T^2 \boldsymbol{p}_T^2}{4M_p^4},$$
$$w_3 \equiv \frac{\boldsymbol{q}_T^2 \boldsymbol{k}_T^2 - 2(\boldsymbol{q}_T \cdot \boldsymbol{k}_T)^2}{2M_p^2 \boldsymbol{q}_T^2}, \quad (5)$$
$$w_4 \equiv 2\left[\frac{\boldsymbol{p}_T \cdot \boldsymbol{k}_T}{2M_p^2} - \frac{(\boldsymbol{p}_T \cdot \boldsymbol{q}_T)(\boldsymbol{k}_T \cdot \boldsymbol{q}_T)}{M_p^2 \boldsymbol{q}_T^2}\right]^2 - \frac{\boldsymbol{p}_T^2 \boldsymbol{k}_T^2}{4M_p^4}.$$

The low $\boldsymbol{p}_T$ part of the TMD distribution functions will inevitably contain nonperturbative hadronic information that needs to be extracted from experimental data, for instance using the proposals in [27,28]. On the other hand, the tails ($\boldsymbol{p}_T \gg M_p$) of the TMDs can be calculated using pQCD and lead to a resummation expression for the angular integrated differential cross section, that is valid for $M_p^2 \ll q_T^2$ and that matches onto the large q_T collinear factorization expression [29–31]. This matching to the large q_T region allows us to extend the TMD expression beyond its range of validity by incorporating the correct power law tail in the TMDs.

To make numerical predictions we will use a functional form for f_1^g which has, in accordance with pQCD, a $1/\boldsymbol{p}_T^2$ tail at large $\boldsymbol{p}_T$ and resembles a Gaussian for small $\boldsymbol{p}_T$,

$$f_1^g(x, \boldsymbol{p}_T^2, \zeta, \mu) = \frac{A_0 M_0^2}{M_0^2 + \boldsymbol{p}_T^2} \exp\left[-\frac{\boldsymbol{p}_T^2}{a\boldsymbol{p}_T^2 + 2\sigma^2}\right], \quad (6)$$

to be considered at $x = M_h/\sqrt{s}$, $\zeta = 1.5\sqrt{s}$, and $\mu = M_h$. As there are no data available on the Higgs transverse momentum distribution, we will fit the parameters in Eq. (6) to the prediction obtained by interfacing the POWHEG [32–34] next-to-leading order gluon fusion calculation [35] to PYTHIA 8.170 [36,37], assuming a Higgs boson mass of 125 GeV and $\sqrt{s} = 8$ TeV. PYTHIA does not take into account effects of gluon polarization, so we fit the data by setting the linearly polarized gluon distribution equal to zero. In this way the TMD prediction without gluon polarization agrees with the PYTHIA prediction. We think this is the most realistic choice we can make, because PYTHIA is tuned to reproduce collider data well. Our Gaussian-with-tail ansatz is able to adequately fit the PYTHIA data, as is shown in Fig. 1. The fit results in the following values for the parameters $\sigma = 38.9$ GeV, $a = 0.555$, and $M_0 = 3.90$ GeV. The absolute size of the cross section will not matter in the relative contributions to be considered below.

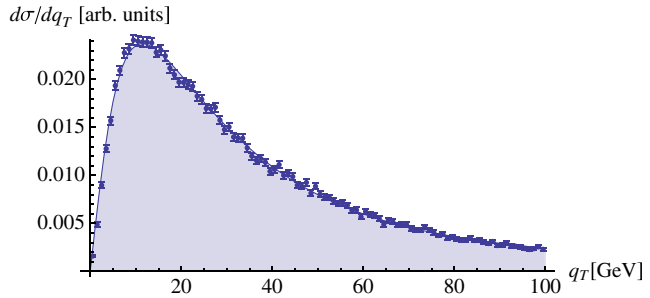

FIG. 1 (color online). Plot of $q_T\mathcal{C}[f_1^g f_1^g]$ (line) and the PYTHIA Higgs $d\sigma/dq_T$ distribution for $M_h = 125$ GeV at $\sqrt{s} = 8$ TeV (points).

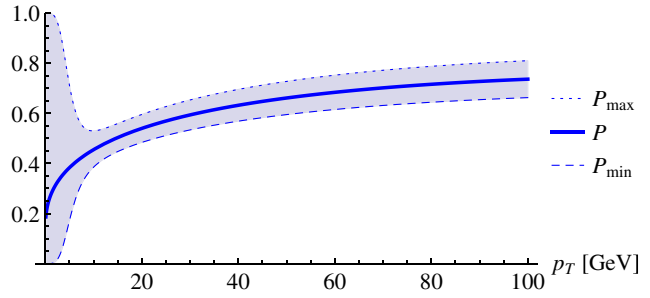

FIG. 2 (color online). Plot of the degrees of polarization $\mathcal{P}_{\min}$, $\mathcal{P}$, and $\mathcal{P}_{\max}$ at $x = M_h/\sqrt{s}$, with $M_h = 125$ GeV and $\sqrt{s} = 8$ TeV.

The linearly polarized gluon distribution will be expressed in terms of the unpolarized gluon distribution and the degree of polarization $\mathcal{P}$, i.e.,

$$h_1^{\perp g}(x, \boldsymbol{p}_T^2, \zeta, \mu) = \mathcal{P}(x, \boldsymbol{p}_T^2, \zeta)\frac{2M_p^2}{\boldsymbol{p}_T^2} f_1^g(x, \boldsymbol{p}_T^2, \zeta, \mu), \quad (7)$$

such that $|\mathcal{P}| = 1$ corresponds to $h_1^{\perp g}$ saturating its upper bound [38] and with the correct power law tail as first calculated in [24]. Alternatively, one could compute the gluon TMDs from the nonpertubative light-front wave functions of the proton; see, e.g., Ref. [39]. Calculations of the gluon TMD distributions at small x using the color glass condensate model predict maximal gluon polarization at large $\boldsymbol{p}_T$ [40].

As it is currently unfeasible to extract the degree of polarization from data, we will calculate it from the large $\boldsymbol{p}_T$ tails of the TMD distributions that can be calculated using pQCD as has been done in Ref. [26] for the unpolarized distribution and Ref. [24] for the linearly polarized gluon distribution. We will follow a similar approach, but keep finite ζ instead of taking the $\zeta \to \infty$ limit and calculate the degree of polarization to leading order in α_s from the MSTW 2008 parton distributions [41] evaluated at a scale of $\mu = 2$ GeV.

The pQCD calculation is only valid in the limit $\boldsymbol{p}_T \gg M_p$. To model the lack of knowledge at low $\boldsymbol{p}_T$, we will define three different degrees of polarization $\mathcal{P}_{\min}$, $\mathcal{P}$, and $\mathcal{P}_{\max}$, of which the first approaches zero at low $\boldsymbol{p}_T$, the second follows the pQCD prediction, and the last reaches up to one at low $\boldsymbol{p}_T$. At high $\boldsymbol{p}_T$, the uncertainty is dominated by the choice of ζ (here determined by varying ζ around 1.5 $\sqrt{s}$ between $\sqrt{s}$ and $2\sqrt{s}$), and the omission of higher order terms. Including all effects we find a conservative estimate of the total uncertainty to be maximally 10%; i.e., we define

$$\begin{aligned}\mathcal{P}_{\min} &\equiv \frac{\boldsymbol{p}_T^4}{p_0^4 + \boldsymbol{p}_T^4} 0.9\mathcal{P}_{\text{pQCD}}(x, \boldsymbol{p}_T^2),\\ \mathcal{P} &\equiv \mathcal{P}_{\text{pQCD}}(x, \boldsymbol{p}_T^2),\\ \mathcal{P}_{\max} &\equiv 1 - \frac{\boldsymbol{p}_T^4}{p_0^4 + \boldsymbol{p}_T^4}[1 - 1.1\mathcal{P}_{\text{pQCD}}(x, \boldsymbol{p}_T^2)],\end{aligned} \quad (8)$$

where $\mathcal{P}_{\text{pQCD}}$ is the pQCD degree of polarization calculated at $\zeta = 1.5\sqrt{s}$ and we take $p_0 = 5$ GeV. The resulting $\mathcal{P}_{\min}$, $\mathcal{P}$ and $\mathcal{P}_{\max}$ are plotted in Fig. 2.

We will consider the partonic process $gg \to X_{0,2} \to \gamma\gamma$ where X is either a spin-0 or spin-2 boson, with completely general couplings. For the interaction vertex we will follow the conventions of Refs. [13,14], where the vertex coupling a spin-0 boson to massless gauge bosons is parametrized as

$$V[X_0 \to V^\mu(q_1)V^\nu(q_2)] = a_1 q^2 g^{\mu\nu} + a_3 \epsilon^{q_1 q_2 \mu\nu}, \quad (9)$$

and for a spin-2 boson as

$$\begin{aligned}&V[X_2^{\alpha\beta} \to V^\mu(q_1)V^\nu(q_2)]\\ &= \frac{1}{2}c_1 q^2 g^{\mu\alpha} g^{\nu\beta} + (c_2 q^2 g^{\mu\nu} + c_5 \epsilon^{q_1 q_2 \mu\nu})\frac{\tilde{q}^\alpha \tilde{q}^\beta}{q^2},\end{aligned} \quad (10)$$

where $q \equiv q_1 + q_2$ and $\tilde{q} \equiv q_1 - q_2$. The coupling to gluons can be different from the coupling to photons, but to keep expressions compact we will consider them equal.

For the $gg \to X_0 \to \gamma\gamma$ subprocess, the nonzero F factors in Eq. (3) read

$$\begin{aligned}F_1 &= 16|a_1|^4 + 8|a_1|^2|a_3|^2 + |a_3|^2,\\ F_2 &= 16|a_1|^4 - |a_3|^4,\end{aligned} \quad (11)$$

and for the $gg \to X_2 \to \gamma\gamma$ process one has

TABLE I. Different spin, parity, and coupling scenarios.

Scenario	0^+	0^-	2_m^+	2_h^+	$2_{h'}^+$	$2_{h''}^+$	2_h^-
a_1	1	0					
a_3	0	1					
c_1			1	0	1	1	0
c_2			$-1/4$	1	1	$-3/2$	0
c_5			0	0	0	0	1

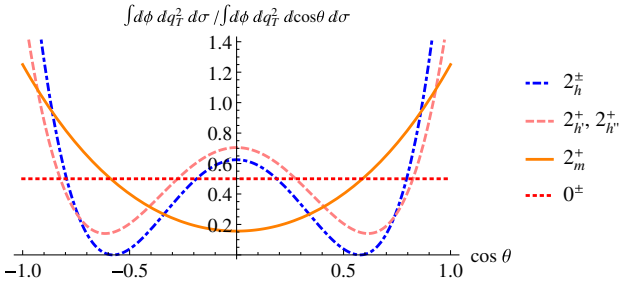

FIG. 3 (color online). Plot of the $\cos\theta$ distribution for the various scenarios.

$$
\begin{aligned}
F_1 &= 18A^+|c_1|^2 s_\theta^4 + (A^+)^2(1-3c_\theta^2)^2 \\
&\quad + \frac{9}{8}|c_1|^4(28c_{2\theta} + c_{4\theta} + 35), \\
F_2 &= 9A^-|c_1|^2 s_\theta^4 + A^-A^+(1-3c_\theta^2)^2, \\
F_3 &= 3s_\theta^2 B^-[3|c_1|^2(c_{2\theta}+3) + A^+(3c_{2\theta}+1)], \\
F_3' &= 6s_\theta^2 \mathrm{Re}(c_1 c_5^*)[3|c_1|^2(c_{2\theta}+3) + A^+(3c_{2\theta}+1)], \\
F_4 &= 9s_\theta^4|c_1|^2[2B^+ + 4|c_5|^2],
\end{aligned} \tag{12}
$$

where we have defined $A^\pm \equiv |c_1 + 4c_2|^2 \pm 4|c_5|^2$, $B^\pm \equiv |c_1 + 2c_2|^2 \pm 4|c_2|^2$, $c_{n\theta} \equiv \cos(n\theta)$, and $s_\theta \equiv \sin(\theta)$. Overall factors have been dropped, because we will be only interested in distributions and not the absolute size of the cross section. Unlike the case for Higgs production from linearly polarized photons [42], there is no direct observable signaling CP violation in the spin-0 case. For the spin-2 case there *is* such a clear signature, being a $\sin 2\phi$ dependence of the cross section, which can only be present if both c_1 and c_5 are nonzero, implying a CP-violating interaction. This $\sin 2\phi$ modulation will have an opposite sign for forward and backward Higgs production though, requiring a separate treatment of those regions.

In Ref. [14] a set of different spin, parity, and coupling scenarios is defined. To those scenarios we will add $2_{h'}^+$ and $2_{h''}^+$, which will serve as examples of higher-dimensional spin-2 coupling hypotheses that are indistinguishable in the θ distribution, but do have a different ϕ distribution. The scenarios are summarized in Table I.

In Fig. 3 we show the diphoton $\cos\theta$ distribution for the various scenarios. In this distribution 0^+ and 0^- are indistinguishable, as are 2_h^+ and 2_h^-, and also $2_{h'}^+$ and $2_{h''}^+$.

In Fig. 4 we show the diphoton transverse momentum distribution for the different coupling hypotheses. The positive parity states show an enhancement at low q_T (< 15 GeV) with respect to the negative parity states. At high q_T (> 15 GeV) this is reversed, but with such a strongly reduced magnitude that it is invisible in the plot. The q_T distribution can thus, in principle, be used to determine the parity of the newly found boson [19,20]. Although the difference is small and most likely difficult to measure experimentally, this is the only way we know to determine the parity in the diphoton channel.

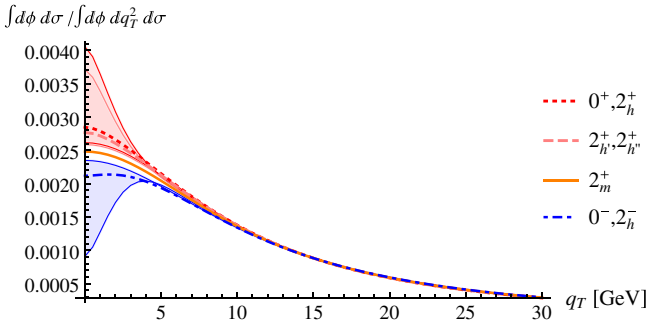

FIG. 4 (color online). Plot of the q_T distribution for the various coupling schemes at $\theta = \pi/2$ and zero rapidity, using an upper limit on the q_T integration in the denominator of $M_h/2$. The shaded area is due to the uncertainty in the degree of polarization.

Figure 5 shows the diphoton ϕ distribution for the selected scenarios. The scalar, pseudoscalar, and $2_h^\pm$ hypotheses show a uniform ϕ distribution, whereas the 2_m^+ has a characteristic $\cos(4\phi)$ dependence with an amplitude of $5.4^{+3.7}_{-1.8}\%$. The $2_{h'}^+$ and $2_{h''}^+$ scenarios exhibit a weak $\cos(4\phi)$ modulation with an amplitude of $1.2^{+0.8}_{-0.4}\%$ and a strong $\cos(2\phi)$ modulation with an amplitude of $24 \pm 3\%$ and opposite sign. The ϕ distribution thus offers a way to distinguish $0^\pm$, 2_m^+, $2_{h'}^+$, and $2_{h''}^+$ from each other, something that is impossible with the $\cos\theta$ distribution alone. Requiring a minimal q_T enhances the effect, but reduces the number of events. A careful optimization of the experimental cuts goes beyond the scope of this Letter. To not go too far outside the range of validity of TMD factorization, we set an upper bound on q_T of $M_h/2$. Without upper bound the size of the effect increases slightly [$\mathcal{O}(10\%)$].

The mass range around the Higgs peak will inevitably contain a large continuum background, which should be carefully subtracted using, e.g., a sideband analysis. Here it should not be assumed that the background is azimuthally isotropic. The $gg \to \gamma\gamma$ continuum production is, for example, also influenced by linear gluon polarization leading to a nonisotropic ϕ distribution [27,43], which for the selected upper bound on the q_T integration is approximately a factor of 3 smaller than on resonance.

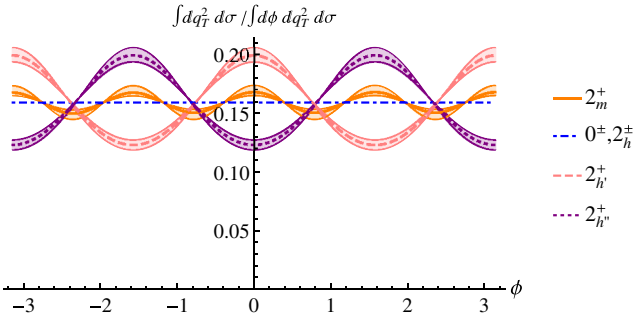

FIG. 5 (color online). Plot of the ϕ distribution for the different benchmark scenarios at $\theta = \pi/2$ and zero rapidity. The shaded area is due to the uncertainty in the degree of polarization.

In conclusion, we have calculated the diphoton distribution in the decay of arbitrary spin-0 and spin-2 bosons produced from gluon fusion, taking into account the fact that gluons inside an unpolarized proton are generally linearly polarized. The gluon polarization brings about a difference in the transverse momentum distribution of positive and negative parity states. At the same time, it causes the azimuthal CS angle ϕ distribution to be nonisotropic for various spin-2 coupling hypotheses. These distributions allow spin and parity scenarios to be distinguished that cannot be done with the polar angle θ dependence alone. We think that these observables could therefore form a valuable addition to the analysis methods to determine the spin, parity, and coupling of the newly found boson at the LHC.

This work was supported in part by the German Bundesministerium für Bildung und Forschung (BMBF), Grant No. 05P12VTCTG.

[1] G. Aad *et al.* (ATLAS Collaboration), Phys. Lett. B **716**, 1 (2012).
[2] S. Chatrchyan *et al.* (CMS Collaboration), Phys. Lett. B **716**, 30 (2012).
[3] http://cds.cern.ch/record/1527124/files/ATLAS-CONF-2013-029.pdf.
[4] http://cds.cern.ch/record/1523699/files/ATLAS-CONF-2013-013.pdf.
[5] http://cds.cern.ch/record/1527127/files/ATLAS-CONF-2013-031.pdf.
[6] S. Chatrchyan *et al.* (CMS Collaboration), Phys. Rev. Lett. **110**, 081803 (2013).
[7] http://cds.cern.ch/record/1523767/files/HIG-13-002-pas.pdf.
[8] http://cds.cern.ch/record/1523673/files/HIG-13-003-pas.pdf.
[9] The coupling of a spin-2 boson to gauge bosons can be realized in multiple ways. We will use the standard notation in which 2_m^+ denotes a spin-2 boson with minimal (lowest dimensional) coupling, which is uniquely defined.
[10] L. D. Landau, Dokl. Akad. Nauk Ser. Fiz. **60**, 207 (1948).
[11] C.-N. Yang, Phys. Rev. **77**, 242 (1950).
[12] S. Y. Choi, D. J. Miller, M. M. Muhlleitner, and P. M. Zerwas, Phys. Lett. B **553**, 61 (2003).
[13] Y. Gao, A. V. Gritsan, Z. Guo, K. Melnikov, M. Schulze, and N. V. Tran, Phys. Rev. D **81**, 075022 (2010).
[14] S. Bolognesi, Y. Gao, A. V. Gritsan, K. Melnikov, M. Schulze, N. V. Tran, and A. Whitbeck, Phys. Rev. D **86**, 095031 (2012).
[15] S. Y. Choi, M. M. Muhlleitner, and P. M. Zerwas, Phys. Lett. B **718**, 1031 (2013).
[16] J. Ellis, R. Fok, D. S. Hwang, V. Sanz, and T. You, arXiv:1210.5229.
[17] The h subscript indicates that the spin-2 boson couples through a higher-dimensional coupling. There are multiple higher-dimensional couplings possible. We follow the convention of Refs. [13,14] for $2_h^{\pm}$.
[18] J. C. Collins and D. E. Soper, Phys. Rev. D **16**, 2219 (1977).
[19] D. Boer, W. J. den Dunnen, C. Pisano, M. Schlegel, and W. Vogelsang, Phys. Rev. Lett. **108**, 032002 (2012).
[20] W. J. den Dunnen, D. Boer, C. Pisano, M. Schlegel, and W. Vogelsang, arXiv:1205.6931.
[21] K. Hagiwara, Q. Li, and K. Mawatari, J. High Energy Phys. 07 (2009) 101.
[22] J. R. Andersen, K. Arnold, and D. Zeppenfeld, J. High Energy Phys. 06 (2010) 091.
[23] J. Frank, M. Rauch, and D. Zeppenfeld, Phys. Rev. D **87**, 055020 (2013).
[24] P. Sun, B.-W. Xiao, and F. Yuan, Phys. Rev. D **84**, 094005 (2011).
[25] J. P. Ma, J. X. Wang, and S. Zhao, arXiv:1211.7144.
[26] X.-d. Ji, J.-P. Ma, and F. Yuan, J. High Energy Phys. 07 (2005) 020.
[27] J.-W. Qiu, M. Schlegel, and W. Vogelsang, Phys. Rev. Lett. **107**, 062001 (2011).
[28] D. Boer, S. J. Brodsky, P. J. Mulders, and C. Pisano, Phys. Rev. Lett. **106**, 132001 (2011).
[29] S. Catani and M. Grazzini, Nucl. Phys. **B845**, 297 (2011).
[30] D. de Florian, G. Ferrera, M. Grazzini, and D. Tommasini, J. High Energy Phys. 06 (2012) 132.
[31] J. Wang, C. S. Li, H. T. Li, Z. Li, and C. P. Yuan, Phys. Rev. D **86**, 094026 (2012).
[32] S. Alioli, P. Nason, C. Oleari, and E. Re, J. High Energy Phys. 04 (2009) 002.
[33] P. Nason, J. High Energy Phys. 11 (2004) 040.
[34] S. Frixione, P. Nason, and C. Oleari, J. High Energy Phys. 11 (2007) 070.
[35] S. Alioli, P. Nason, C. Oleari, and E. Re, J. High Energy Phys. 06 (2010) 043.
[36] T. Sjostrand, S. Mrenna, and P. Z. Skands, J. High Energy Phys. 05 (2006) 026.
[37] T. Sjostrand, S. Mrenna, and P. Z. Skands, Comput. Phys. Commun. **178**, 852 (2008).
[38] P. J. Mulders and J. Rodrigues, Phys. Rev. D **63**, 094021 (2001).
[39] J. R. Forshaw and R. Sandapen, Phys. Rev. Lett. **109**, 081601 (2012).
[40] A. Metz and J. Zhou, Phys. Rev. D **84**, 051503 (2011).
[41] A. D. Martin, W. J. Stirling, R. S. Thorne, and G. Watt, Eur. Phys. J. C **63**, 189 (2009).
[42] B. Grzadkowski and J. F. Gunion, Phys. Lett. B **294**, 361 (1992).
[43] W. J. den Dunnen, Ph.D. thesis, Vrije Universiteit Amsterdam, 2012, http://dare.ubvu.vu.nl/handle/1871/39659.